Acta Neuropathologica (2025) 149:57
https://doi.org/10.1007/s00401-025-02890-7

ORIGINAL PAPER

Immunohistochemical evaluation of a trial of gantenerumab or solanezumab in dominantly inherited Alzheimer disease

Charles D. Chen · Erin E. Franklin · Yan Li · Nelly Joseph-Mathurin · Aime L. Burns · Diana A. Hobbs, et al. ***[full author details at the end of the article]***

Received: 24 February 2025 / Revised: 22 April 2025 / Accepted: 9 May 2025
© The Author(s) 2025

Abstract
Clinical trials of anti-amyloid-β (Aβ) monoclonal antibodies in Alzheimer disease (AD) infer target engagement from Aβ positron emission tomography (PET) and/or fluid biomarkers such as cerebrospinal fluid (CSF) Aβ42/40. However, these biomarkers measure brain Aβ deposits indirectly and/or incompletely. In contrast, neuropathologic assessments allow direct investigation of treatment effects on brain Aβ deposits—and on potentially myriad 'downstream' pathologic features. From a clinical trial of anti-Aβ monoclonal antibodies in dominantly inherited AD (DIAD), in the largest study of its kind, we measured immunohistochemistry area fractions (AFs) for Aβ deposits (10D5), tauopathy (PHF1), microgliosis (IBA1), and astrocytosis (GFAP) in 10 brain regions from 10 trial cases—gantenerumab ($n=4$), solanezumab ($n=4$), placebo/no treatment ($n=2$)—and 10 DIAD observational study cases. Strikingly, in proportion to total drug received, Aβ deposit AFs were significantly lower in the gantenerumab arm versus controls in almost all areas examined, including frontal, temporal, parietal, and occipital cortices, anterior cingulate, hippocampus, caudate, putamen, thalamus, and cerebellar gray matter; only posterior cingulate and cerebellar white matter comparisons were non-significant. In contrast, AFs of tauopathy, microgliosis, and astrocytosis showed no differences across groups. Our results demonstrate with direct histologic evidence that gantenerumab treatment in DIAD can reduce parenchymal Aβ deposits throughout the brain in a dose-dependent manner, suggesting that more complete removal may be possible with earlier and more aggressive treatment regimens. Although AFs of tauopathy, microgliosis, and astrocytosis showed no clear response to partial Aβ removal in this limited autopsy cohort, future examination of these cases with more sensitive techniques (e.g., mass spectrometry) may reveal more subtle 'downstream' effects.

Keywords Clinical trial · Anti-amyloid-β monoclonal antibodies · Alzheimer disease · Digital pathology · PiB PET · CSF

Introduction

Amyloid-β (Aβ) plaques are the neuropathological hallmark of Alzheimer disease (AD) [9, 23, 25, 26, 29, 50]. In dominantly inherited AD (DIAD), rare pathogenic variants in the amyloid precursor protein (*APP*), presenilin-1 (*PSEN1*), and presenilin-2 (*PSEN2*) genes cause an increase in aggregation-prone forms of Aβ peptide [42, 49], fostering aggressive Aβ plaque formation, neuroinflammation, neurofibrillary tangle pathology, synaptic and neuronal losses, and dementia [4, 47]. These observations support the idea that accrual of Aβ is a permissive and required first step in the path to symptomatic AD [14, 44, 56]. In response, many treatment strategies for AD have focused on Aβ as a drug target, spurring the development of several anti-Aβ monoclonal antibody-based therapeutics [27, 33, 37, 51, 55]. Although some earlier clinical trials of anti-Aβ monoclonal antibodies in AD failed to meet their cognitive endpoints, more recent trials have demonstrated that substantial removal of Aβ burden by these agents can slow the rate of cognitive decline [20, 52].

Similarly, in the first clinical trial of the Dominantly Inherited Alzheimer Network Trials Unit (DIAN-TU-001),

Data used in the preparation of this article were obtained from the Dominantly Inherited Alzheimer Network Trials Unit (DIAN-TU). As such, the study team members within the DIAN-TU contributed to the design and implementation of DIAN-TU and/or provided data but may not have participated in the analysis or writing of this report. A complete listing of the DIAN-TU Study Team Members can be found at https://dian.wustl.edu/our-research/funding/.

Author Dr. Francisco Lopera passed away in September, 2024

Published online: 03 June 2025

in which participants with DIAD received an anti-Aβ monoclonal antibody (gantenerumab or solanezumab) or placebo, neither treatment slowed cognitive decline, despite evidence for partial clearance of Aβ burden by gantenerumab (inferred by Aβ positron emission tomography [PET] and cerebrospinal fluid [CSF] biomarkers Aβ42/40, p-tau181, and t-tau) [46]. However, recent pre-specified analyses suggest that DIAN-TU-001 study participants who received the longest dosing regimens of gantenerumab in the trial and the subsequent open label extension period showed far lower beta-amyloid burdens and a delay in symptom onset and clinical progression, with reduced hazard ratios for time to recurrent progression in CDR-SB relative to controls [6]. Although these top responders and most other participants remain alive, a small subset of DIAN-TU-001 participants succumbed to end-stage AD and generously underwent brain donation. To measure the effects of these treatments on Aβ clearance more directly, we examined the first ten postmortem cases from the DIAN-TU-001—recipients of gantenerumab ($n=4$), solanezumab ($n=4$), placebo/no treatment ($n=2$)—and ten postmortem cases from the DIAN Observational Study (DIAN-Obs) using quantitative immunohistochemistry to measure Aβ deposits in ten brain regions. For context, we also compared these results to their corresponding antemortem Aβ PET and CSF biomarker measurements, as well as quantitative immunohistochemical measurements of microgliosis, astrocytosis, and tauopathy.

Materials and methods

Study approval

This study was conducted in accordance with the Declaration of Helsinki (version 7) and the International Conference on Harmonization and Good Clinical Practice guidelines. Protocols for the study have received prior approval by the local Institutional Review Board (IRB) of Ethics Committee of each DIAN site, and by the Washington University IRB for the Knight ADRC. Participants or their caregivers provided written informed consent. The clinical trial registration number is NCT01760005.

Study participants

The first ten postmortem cases of the DIAN-TU-001 were selected for inclusion in this study (Table 1). Investigators were blinded to the drug arm of each DIAN-TU-001 participant (gantenerumab, solanezumab, or placebo).

Ten additional postmortem cases were included from among the brain donor participants in the DIAN-Obs study and from family members of DIAN-Obs participants who were not enrolled in DIAN-Obs, but volunteered for brain donation (Table 1). These ten observational controls were selected for numerical balance and to represent approximately the same proportions of *APP*, *PSEN1*, and *PSEN2* mutations as the first ten postmortem DIAN-TU-001 cases; they also had sufficient high-quality tissue samples available for the immunohistochemical experiments included in this study.

Postmortem neuropathology

Brain tissues were collected at the time of autopsy following an established protocol [12, 15, 16], in which left hemibrains are fixed in 10% neutral-buffered formalin for at least two weeks and right hemibrains are frozen. However, two cases deviated from this protocol; DIAN-Obs Case #3 (see Table 1) was processed with a reversal of standard left and right hemibrain processing, and DIAN-TU-001 Case #6 (see Table 1) was fixed whole in observation of institutional COVID-19 pandemic restrictions at the autopsy site. After formalin fixation, the supratentorial portion of each fixed hemibrain was sliced in the coronal plane; the hemicerebellum, parasagitally; and the hemibrainstem, axially. Tissue samples were taken from up to 16 representative brain regions, then processed in standard fashion for histology of formalin-fixed, paraffin-embedded tissue. Histologic sections were cut at 6-µm thickness and mounted on glass slides. Histologic slides were stained with hematoxylin and eosin and by 3,3′-diaminobenzidine (DAB) immunohistochemistry using antibodies for amyloid-β (10D5, Eli Lilly and Company, Indianapolis, IN, USA, an antibody directed at amyloid-β that also detects amyloid-β-containing full-length APP and APP C99), phosphorylated tau (PHF1, formerly a gift from Dr. Peter Davies, now from Feinstein Institute for Medical Research, Manhasset NY, USA), phosphorylated alpha-synuclein (Cell Applications, San Diego, CA, USA), and phosphorylated TAR DNA binding protein of 43 kDa (TDP-43, Cosmo Bio USA, Carlsbad, CA, USA); for three DIAN-Obs cases, a modified Bielschowsky silver impregnation stain was also applied. Postmortem neuropathologic assessment of cases included a systematic evaluation of histologic slides; AD neuropathologic changes were assessed using criteria described within the National Alzheimer Coordinating Center Neuropathology Diagnosis Coding Guidebook, supplemented by criteria for TDP-43 proteinopathy [31, 39, 40].

In the current study, ten brain regions were ultimately selected for quantitative histologic analysis: the frontal lobe (middle frontal gyrus), temporal lobe (superior and middle temporal gyri), parietal lobe (angular gyrus), occipital lobe (calcarine sulcus and parastriate cortex), hippocampus (in the coronal plane of the lateral geniculate nucleus), caudate and putamen (at or near the coronal plane of the anterior

Table 1 Participant characteristics

	Sex	*APOE*	Family mutation	AAO	Age at baseline	CDR® at baseline	Drug	Days on low dose	Maximum low dose (mg)	Days on high dose	Maximum tolerated high dose (mg)	Drug received by final PET (mg)	Drug received by final CSF (mg)	Total drug received (mg)	Reason for discontinuation (if withdrew from study)
DIAN-TU-001															
1	M	23	*PSEN1*	40–50	50–60	1	Sola	507	400	0	N/A	N/A	4800	7200	Met protocol discontinuation criteria (increased microhemorrhages from baseline)
2	M	34	*APP*	40–50	40–50	0.5	Gant	696	225	0	N/A	2925	2925	5850	Withdrawal by subject or proxy
3	M	33	*PSEN1*	40–50	50–60	1	Sola	1402	400	0	N/A	10,400	10,400	20,400	Withdrawal by subject or proxy
4	M	34	*PSEN1*	40–50	40–50	0.5	Gant	1255	225	520	1200	14,010	14,010	27,045	Withdrawal by subject or proxy
5	M	23	*PSEN1*	40–50	40–50	1	Gant	904	225	1117	900	17,475	17,475	35,400	N/A
6	F	44	*PSEN1*	50–60	50–60	0.5	Placebo	0	0	0	0	0	0	0	N/A
7	F	33	*PSEN1*	20–30	30–40	1	Sola	421	400	0	N/A	6000	5200	6400	Withdrawal by subject or proxy
8	M	33	*PSEN1*	20–30	30–40	1	N/A	0	0	0	0	N/A	N/A	0	N/A
9	F	33	*PSEN1*	30–40	30–40	1	Sola	784	400	645	1600	46,800	46,800	48,400	N/A
10	M	34	*PSEN1*	60–70	50–60	0.5	Gant	787	225	1068	1200	29,220	29,220	48,420	N/A
DIAN-Obs															
1	M	N/A	*PSEN1*	40–50	N/A	N/A	N/A	0	N/A	0	N/A	N/A	N/A	0	N/A
2	M	44	*PSEN1*	30–40	40–50	0.5	N/A	0	N/A	0	N/A	N/A	N/A	0	N/A
3	F	N/A	*PSEN1*	40–50	N/A	N/A	N/A	0	N/A	0	N/A	N/A	N/A	0	N/A
4	F	23	*PSEN1*	40–50	40–50	2	N/A	0	N/A	0	N/A	N/A	N/A	0	N/A
5	M	44	*APP*	50–60	50–60	1	N/A	0	N/A	0	N/A	N/A	N/A	0	N/A
6	F	34	*PSEN1*	30–40	30–40	1	N/A	0	N/A	0	N/A	N/A	N/A	0	N/A
7	M	33	*PSEN1*	40–50	50–60	0.5	N/A	0	N/A	0	N/A	N/A	N/A	0	N/A
8	M	33	*PSEN1*	50–60	50–60	3	N/A	0	N/A	0	N/A	N/A	N/A	0	N/A
9	F	33	*PSEN1*	40–50	40–50	0.5	N/A	0	N/A	0	N/A	N/A	N/A	0	N/A
10	M	33	*PSEN1*	40–50	40–50	0.5	N/A	0	N/A	0	N/A	N/A	N/A	0	N/A

We are limited by DIAN policy from reporting exact age at death, family mutation, and age at onset. DIAN-TU-001 Case #8 was part of the DIAN-TU Cognitive Run-In (CRI) and did not ultimately enroll in a drug arm and thus has limited antemortem data available. DIAN-Obs Cases #1 and #3 were family members of DIAN-Obs participants who consented to brain donation but did not otherwise participate in the study and thus have limited antemortem data available. DIAN-TU-001 Cases #2 and #3 did not have CDR® available immediately prior to death

AAO age at onset (reported as mean AAO for all DIAN participants with that specific mutation), *APOE* Apolipoprotein E, *APP* Aβ precursor protein, *CDR*® Clinical Dementia Rating®, *Gant* Gantenerumab, *PSEN1* presenilin-1, *PSEN2* presenilin-2, *Sola* Solanezumab

commissure), thalamus (including subthalamic nucleus), anterior cingulate gyrus (in the coronal plane of the genu of the corpus callosum), and posterior cingulate gyrus (including precuneus, in the coronal plane of the splenium). Two more brain regions—the cerebellar gray matter and cerebellar white matter—were also selected to measure Aβ deposits in these commonly used reference regions for Aβ PET imaging. To enable quantitative studies of astrocytosis and microgliosis, slides from these brain regions were stained by DAB immunohistochemistry using antibodies for astrocyte marker GFAP (Anti GFAP, Rabbit, Dako, Carpinteria, CA, USA) and microglial marker IBA1 (Anti Iba1, Rabbit, FUJIFILM Wako Pure Chemical Corporation, Richmond, VA, USA). Histologic slides were digitized with a 20× bright-field objective at 0.46 µm/pixel resolution on a Hamamatsu NanoZoomer 2.0-HT slide scanner (Hamamatsu Photonics K.K., Hamamatsu, Japan). Quantification of each digitized slide was performed using QuPath, an open source software for digital pathology [2].

First, for each slide, a tissue region of interest (ROI) was manually delineated according to the following guidelines: for regions sampled from the cerebral cortex (frontal, temporal, parietal, and occipital lobes, and anterior and posterior areas of the cingulate gyrus), a cortical ribbon defined by the pial surface and the gray/white boundary was drawn. For the hippocampus, caudate and putamen, and thalamus, a tissue ROI was drawn according to the Atlas of the Human Brain, 4th edition [36]. For the cerebellum, a gray matter ROI and a white matter tissue ROI were drawn. For all regions, processing artifacts (e.g., bubbles trapped between the coverslip and the tissue sample, or "edge" artifacts wherein non-specific immunohistochemistry staining often occurs at the edges of tissue sections) were excluded. Next, color deconvolution was used to generate DAB, hematoxylin, and residual channels from the original RGB channels of the digitized slide [45]. Then, the StarDist extension for QuPath was used to segment pathologic features of interest from the DAB channel [48]. For 10D5 slides, StarDist was used to segment cored/compact Aβ plaques and cerebral amyloid angiopathy (CAA); for PHF1 slides, neurofibrillary tangles; for GFAP slides, astrocyte cell bodies; and for IBA1 slides, microglia cell bodies. However, cored/compact Aβ plaques and CAA, neurofibrillary tangles, and astrocyte and microglia cell bodies are not the only pathologies present: for 10D5 slides, there can also be diffuse Aβ plaques; for PHF1 slides, there can also be neuropil threads and neuritic plaques; and for GFAP and IBA1 slides, there can also be extensive ramified processes extending from and/or appearing entirely detached from a cell body. Thus, for each slide, the minimum optical density for each segmented Aβ plaque/tau tangle/astrocyte/microglia was found, and the 95th percentile of all such values was used to define the threshold of a pixel classifier. Then the area of each tissue ROI with optical density greater than the defined threshold was divided by the total area of the tissue ROI to generate an area fraction. All analyses were done on 4× downsampled images (1.84 µm/pixel resolution) for efficiency. All segmentations were reviewed by neuropathologist R.J.P. for accuracy.

Antemortem MRI acquisition

Participants were scanned on DIAN-approved 3T MRI scanners [8, 38]. Across all scanners, T1-weighted head MR images were acquired using a magnetization prepared rapid gradient echo generalized autocalibrating partial parallel acquisition sequence with a repetition time = 2300 ms, echo time = 2.95 ms, flip angle = 9°, and voxel resolution = $1.1 \times 1.1 \times 1.2$ mm^3.

Antemortem Aβ PET acquisition

Participants were scanned on DIAN-approved PET scanners [8, 38]. Participants received a single 14.5 ± 2.5 (mean ± standard deviation) mCi intravenous bolus injection of Pittsburgh Compound-B (^{11}C-PiB) at each imaging session. Emission data were collected 40–70 min post injection. List-mode data were reconstructed using ordered subset expectation maximization. A low-dose CT scan preceded PET acquisition for attenuation correction. Reconstructed PET images were processed using the PET Unified Pipeline (https://github.com/ysu001/PUP) [54]. After segmenting MR images into ROIs using FreeSurfer version 5.3 [22], regional standardized value update ratios (SUVRs) were defined from the reconstructed PET images using a cerebellar gray reference region.

Antemortem CSF collection

CSF was collected under standardized operating procedure. Participants underwent lumbar puncture (L4-L5) in the morning following overnight fasting. Twenty to 30 mL of CSF was collected in a 50-mL polypropylene tube via gravity drip using an atraumatic Sprotte 22 gage spinal needle. CSF was kept on ice and centrifuged at low speed within 2 h of collection, then transferred to another 50-mL tube. CSF was aliquoted at 500 µL into polypropylene tubes and stored at -80°C [21]. CSF samples not collected at Washington University in St. Louis but at other USA sites were shipped overnight on dry ice to Washington University in St. Louis, whereas samples collected at non-USA sites were stored at minus 80° C and shipped quarterly on dry ice to Washington University in St. Louis. Prior to analysis, samples were brought to room temperature per manufacturer instructions. Samples were vortexed and transferred to polystyrene cuvettes for analysis.

Concentrations of Aβ40, Aβ42, t-tau, and p-tau181 were measured by chemiluminescent enzyme immunoassay using a fully automated platform (LUMIPULSE G1200, Fujirebio, Malvern, Pennsylvania, USA) according to manufacturer's specifications. Concentrations of p-tau217 and p-tau217 phosphorylation occupancy (pT217/T217) were measured by high-resolution mass spectrometry (HRMS) as previously described [3].

Statistical analysis

Statistical analyses were conducted in R version 4.1.0 [43]. Welch two sample t-tests were used to estimate statistical differences in postmortem neuropathology (Aβ, tau, microglia, and astrocyte area fractions) between either the gantenerumab or solanezumab treatment arms and the control group for each brain region, and p values were adjusted for false discovery rate (FDR) control by the Benjamini–Hochberg procedure [7, 16]. Linear mixed-effects models were used to estimate statistical differences in longitudinal change of antemortem biomarkers (Aβ PET, CSF Aβ42/40, CSF p-tau181, CSF t-tau, CSF p-tau217, and CSF pT217/T217) between either the gantenerumab or solanezumab treatment arms and the control group. The fixed effects were Drug, Time, and their interaction, and the random effects were individual-level random intercepts to account for the correlation across repeated measurements from the same individual over time [17]. For Aβ PET, linear mixed-effects models were used for each brain region, and p values were adjusted for FDR control by the Benjamini–Hochberg procedure [7].

Results

Participant characteristics

Participants in this study were either enrolled in the DIAN-TU-001 gantenerumab arm ($n=4$), the DIAN-TU-001 solanezumab arm ($n=4$), the DIAN-TU-001 placebo arm ($n=1$), the DIAN-TU CRI (Cognitive Run-In, $n=1$), or the DIAN-Obs study ($n=8$), or were a family member of a DIAN-Obs participant ($n=2$). Participants from the last four groups were pooled together to form the control group for the current study ($n=12$).

Imaging-to-pathology comparison: illustrative example

First, to facilitate understanding, we compare Aβ PET imaging and Aβ neuropathology findings for a pair of well-matched participants from the gantenerumab arm (DIAN-TU-001 Case #5 in Table 1) and the placebo arm (DIAN-TU-001 Case #6 in Table 1). By antemortem Aβ PET imaging, the participant in the gantenerumab arm showed a substantial decrease in SUVR in the caudate and putamen over the course of the trial, whereas the participant in the placebo arm showed little to no corresponding decrease (Fig. 1a). Likewise, postmortem Aβ neuropathology revealed a far lower burden of striatal Aβ deposition in this gantenerumab-arm participant compared to their placebo arm counterpart (Fig. 1b–d). Next, we examine changes in longitudinal biomarkers and neuropathologic findings across the rest of the cohort.

Longitudinal changes in antemortem biomarkers

In the greater DIAN-TU-001 trial, participants in the gantenerumab arm showed evidence of longitudinal reductions of Aβ burden, as measured by Aβ PET and CSF biomarkers Aβ42/40, p-tau181, and t-tau; participants in the solanezumab arm did not [46]. To determine whether the participants included in our smaller study might accurately represent this larger DIAN-TU-001 trial cohort, and whether our control group might adequately mimic the DIAN-TU-001 placebo arm, we examined and compared their antemortem biomarker measurements.

Longitudinal changes in regional Aβ PET SUVR of participants in the gantenerumab arm, the solanezumab arm, and the control group are presented in Fig. 2a. Note that five participants in the control group and one participant in the solanezumab arm do not have PET-imaging data, because they enrolled in the trial when no study drug was available (DIAN-TU CRI, $n=1$), or they were family members of DIAN-Obs participants who consented to brain donation but did not otherwise participate in the study ($n=2$), or their PET-imaging session failed quality control ($n=3$). In general, consistent with composite findings from the larger cohort [46], the regional Aβ PET SUVRs of participants in the gantenerumab arm decreased more rapidly than those of the control group, with decreases in temporal cortex, caudate, putamen, and thalamus reaching significance. It is worth noting, however, that these Aβ PET SUVR results were obtained with cerebellar gray matter as the reference region—a standard approach for studies of sporadic or late-onset AD. In previous work, we have shown that, in DIAD, cerebellar gray often harbors substantial Aβ deposits, and its use as a reference region may lead to underestimation of amyloid burden in Aβ PET studies [46]. With cerebellar white matter used as an alternative reference region for our smaller cohort, regional effect sizes were larger and the gantenerumab-associated decrease in the anterior cingulate SUVR reached significance (Supplementary Fig. 2). Also consistent with composite findings from the larger cohort, regional Aβ PET SUVRs of the solanezumab arm

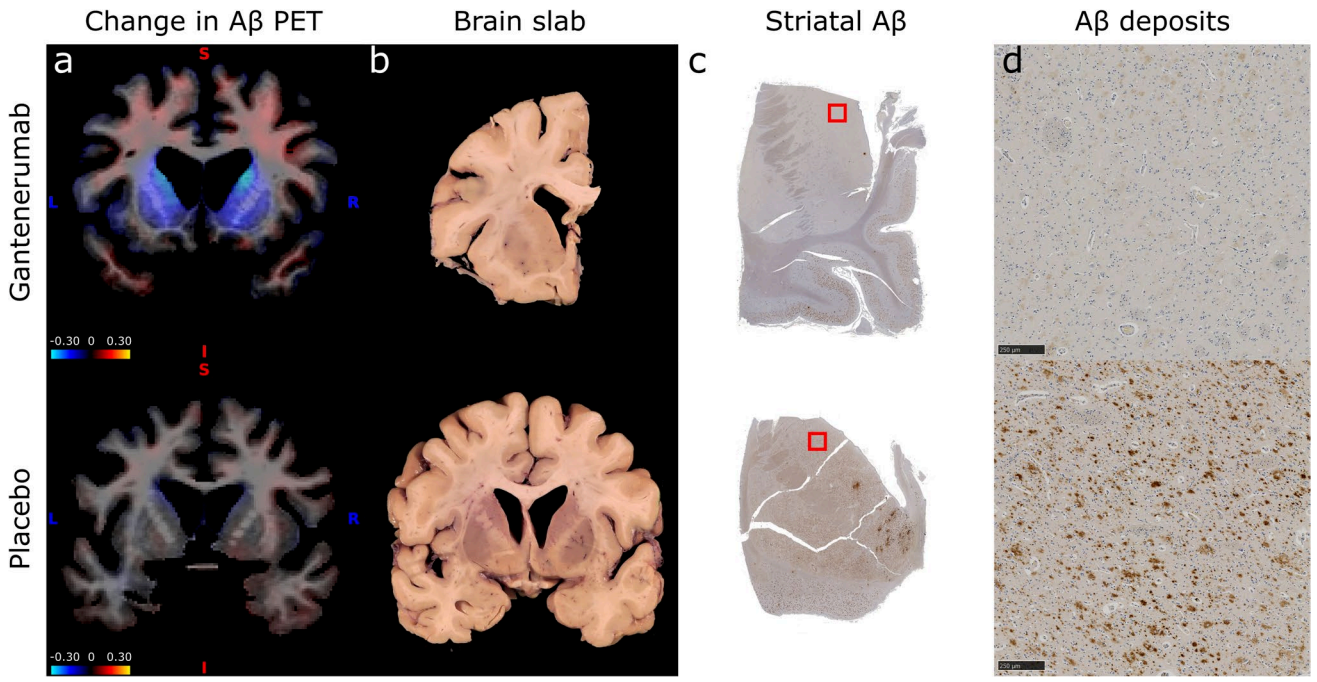

Fig. 1 An exemplar imaging-neuropathology comparison. (**a**) Aβ PET imaging from a participant in the gantenerumab arm (top row, DIAN-TU-001 Case #5 in Table 1) and a participant in the placebo arm (bottom row, DIAN-TU-001 Case #6 in Table 1) showing annualized increases (red) and decreases (blue) in SUVR over the course of the trial in the caudate and putamen (here shown near the coronal plane of the anterior commissure). (**b**) Corresponding coronal slices from the participants' brain donations after formalin-fixation. Differences in ventricularvolume between antemortem imaging and postmortem photography are due to ex vivo fixation. (**c**) Digitized sixmicron histology sections representing the caudate and putamen from both participants, batch-stained with standard DAB immunohistochemistry for Aβ (10D5 antibody). The red square indicates the location of the detail shown in the next panel. (**d**) Detail of the 10D5 staining. Scale bars are 250 µm

participants generally decreased, but without significant differences from controls, regardless of reference region used.

Longitudinal changes in CSF Aβ42/40, p-tau181, t-tau, p-tau217, and pT217/T217 are presented in Fig. 2b. Note that five participants in the control group do not have longitudinal CSF biomarker data, because they enrolled in the trial when no study drug was available (DIAN-TU CRI, $n=1$), or they were family members of DIAN-Obs participants who consented to brain donation but did not otherwise participate in the study ($n=2$), or they had only one visit with CSF collection ($n=2$). Nevertheless, generally consistent with findings from the larger DIAN-TU-001 cohort, CSF Aβ42/40 increased (p value = 0.0002; suggestive of lower burdens of Aβ plaques [21] and/or protofibrils [1]) and CSF t-tau decreased (p value = 0.024) more rapidly in our gantenerumab-arm participants than in our control group; CSF p-tau181, p-tau217, and pT217/T217 also decreased, but did not reach significance (p values = 0.071, 0.18, 0.88, respectively). In the solanezumab arm, longitudinal changes in CSF t-tau and CSF p-tau181 did not differ significantly from controls; CSF p-tau217 and pT217/T217 decreased more rapidly than in the control group, but CSF p-tau217 did not reach significance (CSF p-tau217 p value-0.056; CSF pT217/T217 p value = 0.017); CSF Aβ42/40 measurements were not available for the solanezumab arm participants in our study ($n=4$).

Postmortem Aβ neuropathology

In kind with the illustrative case pairing described in Fig. 1, the regional Aβ deposit area fractions of the gantenerumab-arm participant group were significantly lower than those of the control group in the caudate and putamen, but they were also lower in the frontal, temporal, parietal, and occipital cortices, hippocampus, thalamus, cerebellar gray matter, and anterior cingulate (Fig. 3a). Although Aβ deposit area fractions of participants in the solanezumab arm appeared qualitatively lower than those of the control group in some brain regions, no brain region showed a statistically significant difference between the solanezumab arm and controls.

By classic neuropathologic classification, only DIAN-TU-001 Case #5 (featured in Fig. 1) qualified for Thal phase 3, reflecting an essential absence of Aβ plaques from diagnostic slides from striatum, thalamus, brainstem, and cerebellum; all other gantenerumab-arm cases, as well as all solanezumab arm cases and control cases, showed robust Aβ

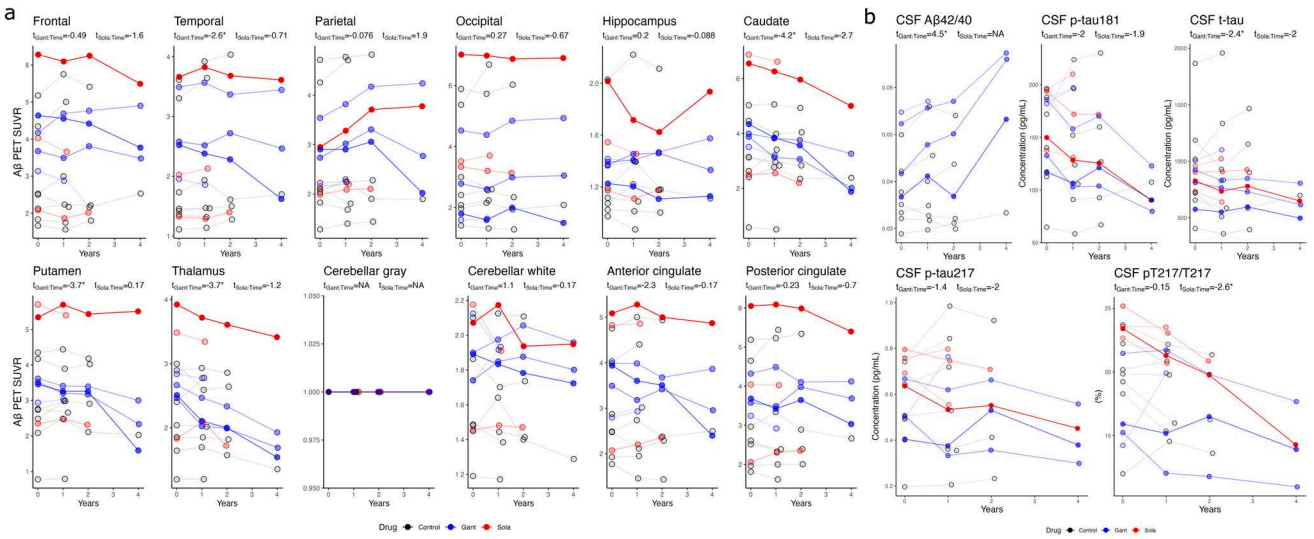

Fig. 2 Longitudinal change in Aβ PET and CSF biomarkers. (**a**) Longitudinal change in regional Aβ PET SUVRs in the gantenerumab arm (blue, n=4), control group (black, n=7), and solanezumab arm (red, n=3). The transparency of each dot corresponds to the total drug received by the time of the final Aβ PET (darker colors represent higher doses; exact dose values can be found in Table 1). (**b**) Longitudinal change in CSF Aβ42/40, ptau181, and t-tau in the gantenerumab arm (blue, n=4), control group (black, n=7), and solanezumab arm (red, n=4). The transparency of each dot corresponds to the total drug received by the time of the final CSF (darker colors represent higher doses; exact dose values can be found in Table 1). Note that there are no participants from the solanezumab group (n=4) with CSF Aβ42/40 measurements available for this study. Also note that five participants from the control group did not have longitudinal CSF measurements, so, for all comparisons, there is an n=7 for the control group. Asterisks denote p-values < 0.05 (*) associated with the t-value of the Gant:Time interaction term in the linear mixed-effects model Outcome~Drug*Time+(1|Case); no Sola:Time interaction was significant. Abbreviations: Gant=Gantenerumab, Sola=Solanezumab

plaques in these regions, meeting criteria for Thal phase 5. CERAD NP scores (based on the regionally maximal density of tau-immunoreactive and/or argyrophilic neuritic plaques in middle frontal gyrus, superior/middle temporal gyri, and angular gyrus) did not differ at all among the gantenerumab, solanezumab, and control groups (Table 2). Likewise, global CAA severity did not differ between the gantenerumab arm and control group (W-value = 18, p value = 0.49, Wilcoxon rank-sum test), nor between the solanezumab arm and control group (W-value = 25, p value = 0.95, Wilcoxon rank-sum test).

Gantenerumab dose response

Beyond a significant reduction in response to gantenerumab treatment, the Aβ area fractions in some brain regions—notably, caudate and putamen—appeared to show a dose-dependent response (Figs. 3a-c). To explore this possibility further, we examined the relationship between cumulative gantenerumab dose and global Aβ burden at the time of antemortem Aβ PET and, later, at autopsy. Although cumulative gantenerumab dose received before the final Aβ PET visit showed no significant linear relationship with Centiloid values (Fig. 3d), the much larger range of cumulative gantenerumab doses received by the time of postmortem assessment (approaching 50,000 mg for one participant) did show a statistically significant linear relationship with Aβ area fractions across all brain regions (t-value = −2.3, p value = 0.036, Fig. 3e), suggesting that Aβ deposit clearance by gantenerumab is, indeed, dose dependent. This result holds even after removing the caudate and putamen data points identified as outliers in Fig. 3a (t-value = −2.2, p value = 0.049).

Postmortem tau, microglia, and astrocyte neuropathology

Given our immunohistochemical evidence for incomplete but widespread and regionally substantial Aβ clearance in response to gantenerumab treatment, we applied a similar immunohistochemical approach to evaluate whether several other major neuropathological features of Alzheimer disease (tauopathy, microgliosis, astrocytosis), considered to be "downstream" of amyloid deposition, were also affected by gantenerumab treatment. In this cohort, no regional tau, microglia, or astrocyte area fraction was significantly lower in the gantenerumab or solanezumab arms compared to the control group (supplementary Figs. 3, 4, and 5, respectively).

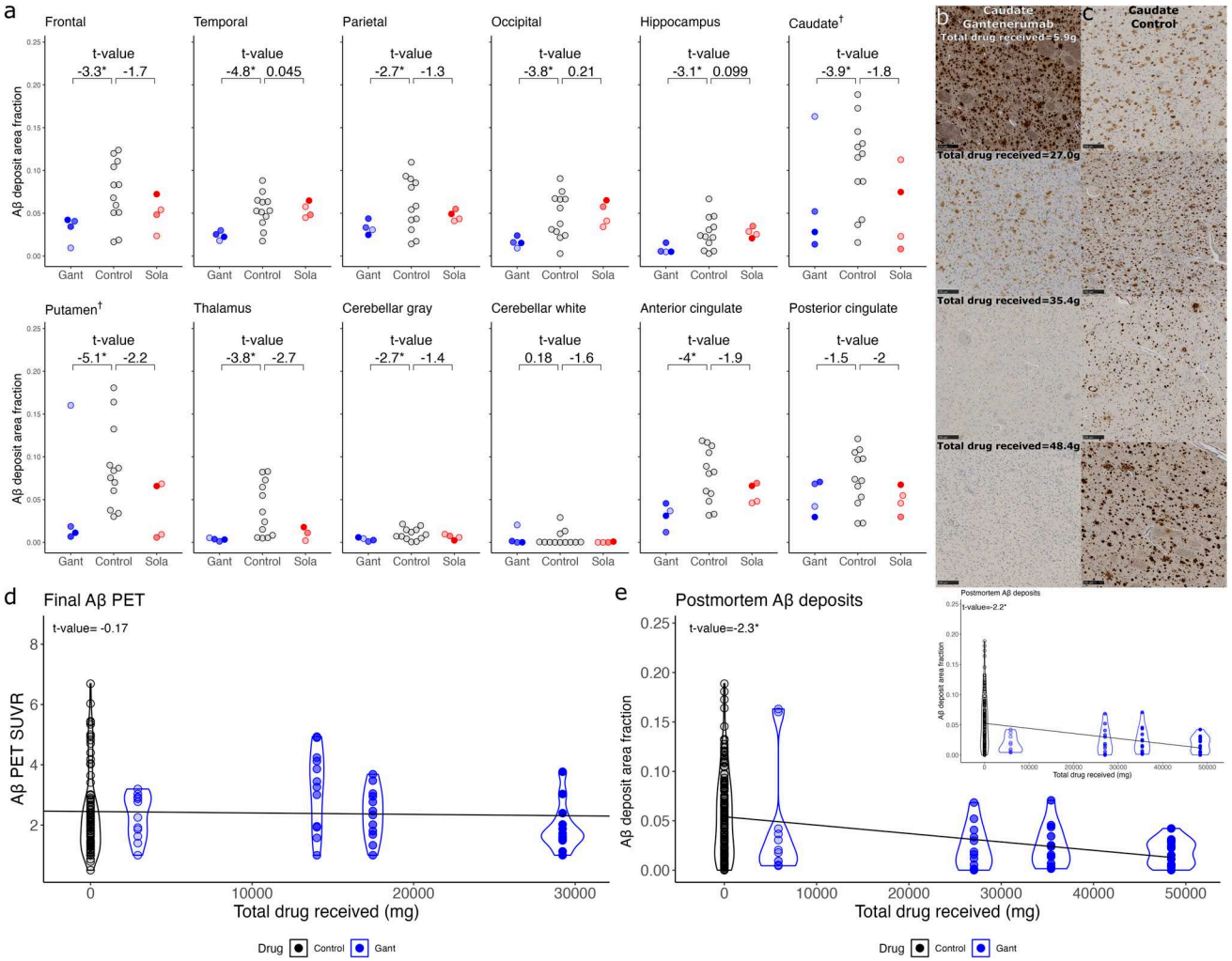

Fig. 3 Aβ deposits and Gantenerumab dose-response. (**a**) Regional Aβ area fractions in the gantenerumab arm (blue, n=4), control group (black, n=12), and solanezumab arm (red, n=4). The transparency of each datapoint corresponds to the total drug dose received at that point in time (darker colors represent higher doses; exact dose values can be found in Table 1). For thalamus, data were available from only three participants from the solanezumab arm. †One participant from the gantenerumab arm with comparatively very high levels of Aβ deposition in the caudate and putamen (over 1.5 times the interquartile range above the third quartile) was treated as an outlier for the statistical comparison versus controls in the caudate and putamen. (**b**) Detail of digitized 10D5 slides of the caudate (location approximates the red square in Fig. 1) from the four gantenerumab-treated participants sorted from lowest total drug received (top) to highest (bottom). (**c**) Detail of digitized 10D5 slides of the caudate from four participants from the control group, approximately matched to the gantenerumab-treated participants on the basis of family mutation [49] and age at death (Supplementary Table 1). Scale bars are 250 µm. Whole-mount images of slides from which photomicrographs in b and c were taken are shown in Supplementary Fig. 1. Asterisks denote p-values < 0.05 (*) associated with Welch two-sample t-tests comparing Aβ area fractions between the control group and the gantenerumab arm or the solanezumab arm. Abbreviations: Gant=gantenerumab, Sola=solanezumab. Gantenerumab dose response at (**d**) final Aβ PET visit and (**e**) postmortem Aβ (10D5) neuropathologic assessment (inset shows results with outliers removed). The transparency of each datapoint corresponds to the total drug dose received at that point in time (darker colors represent higher doses). Asterisks denote p-values < 0.05 (*) associated with the t-value of the Dose term in the linear mixed-effects model Outcome~Dose+(1|Case), where Outcome is Aβ PET SUVR or Aβ area fraction, Dose is a fixed effect term indicating the cumulative dose of gantenerumab received for each case, and Case is a random intercept term

Discussion

In this largest autopsy study to date of individuals treated with anti-Aβ monoclonal antibodies, we provide direct immunohistochemical evidence of gantenerumab-mediated Aβ deposit removal, complementing and extending the timeline and dosage monitored by antemortem Aβ PET and CSF biomarkers during the DIAN-TU-001 trial [46].

Because gantenerumab dosage was adjusted upwards relatively late in the trial [44, 55] and administration continued after final Aβ PET, a few of our autopsied participants received far greater cumulative doses by the time

Table 2 Participant postmortem neuropathology

	Age at death	Final CDR®	Drug	Interval between last dose and death (years)	Interval between last Aβ PET and death (years)	Thal phase	Braak NFT stage	CERAD NP score	CAA	LBD	Additional postmortem findings
DIAN-TU-001											
1	50–60	3	Sola	2	N/A	5	V	3	3	Amygdala	0
2	50–60	2	Gant	2	3	5	VI	3	1–2	Limbic, brain stem sparing	Arteriosclerosis 2–3
3	60–70	2	Sola	1	3	5	VI	3	3	0	Arteriosclerosis 1
4	40–50	3	Gant	2	2	5	VI	3	1–2	Amygdala	0
5	50–60	3	Gant	0	1	3	VI	3	2	0	0
6	50–60	3	Placebo	N/A	1	5	VI	3	3	Limbic, brain stem sparing	TDP-43 1; cortical microinfarct
7	40–50	3	Sola	3	2	5	VI	3	1; 3 in cerebellum	Neocortical	0
8	30–40	3	N/A	N/A	N/A	5	VI	3	1–2; 3 in cerebellum	Amygdala	Acute/subacute perivascular white matter hemorrhages
9	40–50	3	Sola	1	1	5	VI	3	1	Amygdala	Arteriosclerosis 1
10	60–70	3	Gant	2	3	5	VI	3	2–3	Limbic	TDP-43 2; ARTAG; arteriosclerosis 1–2; vascular mineralization
DIAN-Obs											
1	40–50	3	N/A	N/A	N/A	5	VI	3	2–3	0	Arteriosclerosis 1
2	40–50	3	N/A	N/A	0	5	VI	3	2	Neocortical	Glioblastoma; arteriosclerosis 1
3	60–70	3	N/A	N/A	N/A	5	VI	3	2–3	Neocortical	Arteriosclerosis 1–2
4	40–50	3	N/A	N/A	1	5	VI	3	1	0	0
5	50–60	3	N/A	N/A	3	5	VI	3	2	Limbic, brain stem sparing	Arteriosclerosis 1
6	40–50	3	N/A	N/A	2	5	VI	3	2–3	Limbic, brain stem sparing	0
7	50–60	3	N/A	N/A	1	5	VI	3	2–3	0	Arteriosclerosis 1
8	60–70	3	N/A	N/A	N/A	5	VI	3	1	0	Arteriosclerosis 1
9	40–50	3	N/A	N/A	2	5	VI	3	2	Lewy neurites only in olfactory peduncle and olfactory tract	0

Table 2 (continued)

	Age at death	Final CDR®	Drug	Interval between last dose and death (years)	Interval between last Aβ PET and death (years)	Thal phase	Braak NFT stage	CERAD NP score	CAA	LBD	Additional postmortem findings
10	50–60	3	N/A	N/A	8	5	VI	3	2–3	0	Multifocal subacute/remote intravascular thrombosis; remote microinfarct/microbleed; arteriosclerosis, 2; vascular mineralization in pallidum

We are limited by DIAN policy from reporting exact age at death, family mutation, and age at onset. DIAN-TU-001 Case #8 was part of the DIAN-TU Cognitive Run-In (CRI) and did not ultimately enroll in a drug arm and thus has limited antemortem data available. DIAN-Obs Cases #1 and #3 were family members of DIAN-Obs participants who consented to brain donation but did not otherwise participate in the study and thus have limited antemortem data available. DIAN-TU-001 Cases #2 and #3 did not have CDR® available immediately prior to death

ARTAG aging-related tau astrogliopathy, *CAA* cerebral amyloid angiopathy, *CDR®* Clinical Dementia Rating®, *LBD* Lewy body dementia, *NFT* neurofibrillary tangle, *NP* neuritic plaque

Severity rating for CAA and arterio-/arteriolo-sclerosis: 1 = very mild/mild; 2 = moderate; 3 = severe. Numerical staging scheme for TDP-43 proteinopathy after [31]

of brain donation than they had received at the time of Aβ PET. This may account for the finding of more widespread Aβ deposit removal at autopsy (eight/ten brain regions) versus Aβ PET (five/ten brain regions). In addition, our gantenerumab participants represented a broad range of four different cumulative dosages at each of the two timepoints; at least in part, this may account for the wide range of Aβ burden observed among the four gantenerumab recipients—most notably within the caudate and putamen but also more broadly, across all ten brain regions combined. Together, these findings of variability suggest (1) that some brain regions may be more readily cleared of Aβ deposits than others, (2) that Aβ deposit removal is dose-dependent, and (3) that greater clearance of Aβ deposits may be possible with sustained high doses over a longer period—as has also recently been confirmed through pre-specified analyses of biomarker measurements from living DIAN-TU-001 participants treated with sustained high doses of gantenerumab during the open label extension of DIAN-TU-001 [6]. We also acknowledge that some gantenerumab-arm participants may have re-accumulated Aβ deposits during the interval between drug discontinuation and death (0 years for Case #5; 2 years for Cases #2, #4, and #10), and that such re-accumulation may have been greater in some than in others. Importantly, this possibility of re-accumulation does not undermine the conclusions above; if anything, it suggests that the treatment-associated nadir of Aβ deposit burden in these participants may actually have been lower than what was measured at autopsy.

Our findings also illustrate the value of applying a quantitative histologic approach to postmortem studies like this one. Classic neuropathologic staging systems for Aβ plaque pathology (e.g., Thal phase and CERAD NP score) are extremely valuable for categorizing cases of ADNC [29] and may be able to register the large reductions in Aβ plaque distribution/density that seem to be required for clinical benefit, but they lack sensitivity for small differences and show "low ceiling" effects; indeed, they did not effectively represent the clear significant differences between groups in this study of DIAD participants.

In addition to confirming target engagement with 'gold-standard' neuropathology, this study began to explore downstream effects of antibody-mediated Aβ removal using quantitative immunohistochemistry for tauopathy, microgliosis and astrocytosis. In AD, tauopathy correlates more closely with cognitive decline than does Aβ plaque burden [10, 11, 24], and astrocytes and microglia play important roles in both AD pathogenesis and antibody-mediated clearance of Aβ deposits [18, 19]. Given that Aβ removal was incomplete and cognitive endpoints were not reached in the DIAN-TU-001 cohort during the trial, it may not surprise that area fractions of tauopathy,

microgliosis, and astrocytosis did not differ between treatment arms and the control group in this study.

Nevertheless, it is worth considering that area fractions of GFAP and IBA1 immunohistochemistry preparations measure only one of the myriad changes that astrocytes and microglia [30] undergo in AD. Future evaluations of glial features such as activation states, cytokine production, etc., may identify truly salient differences between gantenerumab-treated and control groups. It may also be worth considering that other neurodegenerative features, such as synaptic/neuronal losses, may be more relevant than tauopathy for monitoring downstream effects of Aβ plaque clearance, because synaptic/neuronal losses correlate even more closely with cognitive decline. Although such analyses are beyond the scope of this preliminary study, evaluation of this autopsy cohort with a broad range of techniques (e.g., proteomics, snRNA seq) might identify important regional changes associated with gantenerumab-mediated amyloid clearance, even if Aβ plaque clearance was incomplete and slowing of cognitive decline was not observed within this autopsy cohort.

Recently, other anti-Aβ antibody therapies have been reported to remove Aβ deposits and slow cognitive decline in sporadic AD [20, 52]. Further, those with the most complete Aβ plaque removal also showed the clearest clinical and cognitive benefits [34]. From that perspective, it is appealing to wonder if higher doses of gantenerumab, sufficiently maintained, could have a measurable effect on cognitive decline—and, perhaps, also on gliosis and tauopathy. To that point, recent pre-specified evaluation of DIAN-TU-001 participants who received the largest cumulative doses of gantenerumab and who showed the greatest reduction of Aβ burden, does suggest a delay in symptom onset and clinical progression, with reduced hazard ratios for time to recurrent progression in CDR-SB relative to controls [6]. Clearly, future AD clinical trials would benefit from a more comprehensive understanding of the pathophysiological processes that are altered by anti-Aβ antibody therapies and associated with their therapeutic effects [32]. Some pathophysiological alterations may be gleaned from antemortem biomarker studies; other alterations that can only be evaluated using tissue must wait until relevant brain donations become available.

Despite its valuable findings, this study has limitations. For example, the death rate within the DIAN-TU-001 cohort limited the DIAN-TU-001 participant number for this study to $n = 10$, and only one of these ten had been assigned to the placebo arm; to create a control group for this study, specimens from one DIAN-TU CRI participant, several DIAN-Obs participants, and a few DIAN-Obs family members were carefully selected for inclusion from among existing DIAN-Obs study brain donors.

Nevertheless, the Aβ PET and CSF biomarker data from this study's included participants do resemble those of their DIAN-TU-001 cohorts of origin and the DIAN-TU-001 placebo group, suggesting that they adequately represent at least these key features of the larger groups in DIAN-TU-001. Perhaps even more important: despite its limited cohort size, this study found statistically significant reductions in regional Aβ area fractions that align with the corresponding CSF and Aβ PET biomarker-based findings.

In any case, the small size of this study is not unusual or unexpected, given the scientific context; most anti-Aβ monoclonal antibody clinical trials are fairly recent, have not benefitted from a sustained, centralized brain donation program, and have not yielded sufficient participant brain donations to support a study of even this modest size. To our knowledge, among all anti-Aβ monoclonal antibody clinical trials, there have only been a few postmortem studies presented or published to date: one participant previously treated with aducanumab from the PRIME Phase 1b study was assessed [41]. Another study has been presented at a conference [35]: one participant previously treated with bapineuzumab from the AAB-001 Phase IIA trial was assessed. Interestingly, the presenters found, similarly to us, that the striatum of their participant had only a few scattered areas of Aβ deposition; this common feature of apparent striatal Aβ clearance in both our study and the bapineuzumab report may be worth investigating further. Finally, more recently, three participants previously treated with lecanemab were assessed [13, 28, 53]. Thus, as the largest human neuropathology study of passive anti-Aβ monoclonal immunotherapy to date, this work is truly unique.

A second potential limitation is that the treatment regimens of the DIAN-TU-001 participants included in this study were heterogeneous. Among the participants in the gantenerumab or solanezumab arms, one participant met protocol discontinuation criteria, and four others withdrew early from the trial, either at their own behest or that of their proxy. Thus, several of the participants in this study did not receive all their scheduled doses and, importantly, they spent little or no time receiving drugs at high dose, as dose escalation occurred midway through the DIAN-TU-001 trial [46, 57]. Although this circumstance did allow analyses of dose-effects for gantenerumab (discussed above), it also likely prevented a fair histologic evaluation of gantenerumab's full potential to remove Aβ deposits, and to change other neuropathologic features such as tauopathy and gliosis.

In addition, these first two limitations (low number of participants, heterogeneous dosing) introduced a statistical susceptibility to outliers. Within the gantenerumab arm, one participant (who received a low total dose of gantenerumab) expired with a dense burden of Aβ deposits in the caudate

and putamen relative to the others (over 1.5 times the interquartile range above the third quartile). Future work is needed to understand whether this outlier's high Aβ burden reflects biologic factors (e.g., a DIAD mutation with inherently abundant striatal Aβ deposition), having received the lowest cumulative gantenerumab dose, and/or technical factors that are not prevented by immunohistochemistry batch-staining.

In summary, this postmortem study corroborates the major findings reported for the DIAN-TU-001 trial: gantenerumab treatment in DIAN-TU-001 engaged its target [5] and reduced burdens of parenchymal Aβ deposits in a dose-dependent fashion, likely to levels lower than those measured during the trial's last Aβ PET measurements. However, Aβ deposit clearance remained incomplete, even for participants who received the highest cumulative doses of gantenerumab, and quantitative immunohistochemical assessments of tauopathy, microgliosis, and astrocytosis did not find significant differences between the treatment arms and controls. Based on these findings, we anticipate that higher cumulative doses, more effective antibodies, and earlier intervention with anti-Aβ antibodies may be more effective in removing or inhibiting the formation of amyloid plaques. We also expect that future postmortem studies, using more sophisticated molecular techniques, will identify changes linking Aβ deposit clearance to slowed cognitive decline. Regardless, in view of other recent encouraging anti-Aβ antibody clinical trial results and the urgent need for further therapeutic improvements, we anticipate that combining more effective anti-Aβ therapies with other treatments, such as anti-tau antibodies or drugs that target other aspects of pathophysiology, will represent promising next steps for AD clinical trials.

Supplementary Information The online version contains supplementary material available at https://doi.org/10.1007/s00401-025-02890-7.

Acknowledgements We gratefully acknowledge the outstanding commitment of the participants, family members, and caregivers whose participation was critical to the success of the DIAN-Obs and DIAN-TU trial. We thank the DIAN-Obs and DIAN-TU study teams for their exceptional dedication and amazing accomplishments which ensured the success of the trial. We appreciate the robust intellectual collaboration between the DIAN-TU investigators, patients and family members, Roche/Genentech, and Eli Lilly & Co., the DIAN-TU Pharma Consortium, the NIH, and regulatory representatives who were critical in making this study possible. We thank the Alzheimer's Association, GHR Foundation, Anonymous Organization, industry partners (Avid Radiopharmaceuticals [a wholly owned subsidiary of Eli Lilly & Co.], Signet, Cogstate), and regulatory representatives for their support. Data collection and sharing for this project were supported by The Dominantly Inherited Alzheimer Network (DIAN, U19AG032438) funded by the National Institute on Aging (NIA), the Alzheimer's Association (SG-20-690363-DIAN), the German Center for Neurodegenerative Diseases (DZNE), the Raul Carrea Institute for Neurological Research (FLENI), the Research and Development Grants for Dementia from Japan Agency for Medical Research and Development (AMED), the Korea Dementia Research Project (HU21C0066) through the Korea Dementia Research Center, funded by the Ministry of Health and Welfare and Ministry of Science and ICT, Republic of Korea, the Spanish Institute of Health Carlos III (ISCIII), the Canadian Institutes of Health Research (CIHR), the Canadian Consortium of Neurodegeneration and Aging, the Brain Canada Foundation, and Fonds de Recherche du Québec – Santé. This manuscript has been reviewed by DIAN Study investigators for scientific content and consistency of data interpretation with previous DIAN Study publications. We acknowledge the altruism of the participants and their families and contributions of the DIAN research and support staff at each of the participating sites for their contributions to this study:

Randall J. Bateman, Alisha J. Daniels, Laura Courtney, Eric McDade, Jorge J. Llibre-Guerra, Charlene Supnet-Bell, Chengie Xiong, Xiong Xu, Ruijin Lu, Guoqiao Wang, Yan Li, Emily Gremminger, Richard J. Perrin, Erin E. Franklin, Laura Ibanez, Gina Jerome, Elizabeth Herries, Jennifer Stauber, Bryce Baker, Matthew Minton, Carlos Cruchaga, Alison M. Goate, Alan E. Renton, Danielle M. Picarello, Tammie Benzinger, Brian A. Gordon, Russell Hornbeck, Jason Hassenstab, Jennifer Smith, Sarah Stout, Andrew J. Aschenbrenner, Celeste M. Karch, Jacob Marsh, John C. Morris, David M. Holtzman, Nicolas Barthelemy, Jinbin Xu, James M. Noble, Sarah B. Berman, Snezana Ikonomovic, Neelesh K. Nadkarni, Gregory S. Day, Neill R. Graff-Radford, Martin Farlow, Jasmeer P. Chhatwal, Takeshi Ikeuchi, Kensaku Kasuga, Yoshiki Niimi, Edward D. Huey, Stephen Salloway, Peter R. Schofield, William S. Brooks, Jacob A. Bechara, Ralph Martins, Nick C. Fox, David M. Cash, Natalie S. Ryan, Mathias Jucker, Christoph Laske, Anna Hofmann, Elke Kuder-Buletta, Susanne Graber-Sultan, Ulrike Obermueller, Johannes Levin, Yvonne Roedenbeck, Jonathan Vöglein, Jae-Hong Lee, Jee Hoon Roh, Raquel Sanchez-Valle, Pedro Rosa-Neto, Ricardo F. Allegri, Patricio Chrem Mendez, Ezequiel Surace, Silvia Vazquez, Francisco Lopera, Yudy Milena Leon, Laura Ramirez, David Aguillon, Allan I. Levey, Erik C. B. Johnson, Nicholas T. Seyfried, John Ringman, Anne M. Fagan, Hiroshi Mori.

Author contributions C.D.C. and R.J.P. wrote the main manuscript text and C.D.C. prepared the figures. All authors reviewed the manuscript critically for important intellectual content.

Funding Charles Chen received support from the Knight ADRC T32 Fellowship (5T32AG058518-04) and the NSF GRFP (DGE-1745038, DGE-2139839). Nelly Joseph-Mathurin received support from the NIH/NIA (1K01AG080123-01). Julia Kofler received support from NIA P30 AG066468. Francisco Lopera received support from NIH (API Colombia), COLBOS, Enroll-HD, Large-PD, and Biogen. John Morris received support from the NIH (P30 AG066444, P01 AG003991, P01 AG026276, U19 AG032438). Richard Perrin received support relevant to this study from the NIH (P30 AG066444, P01 AG003991, P01 AG026276, U19 AG032438, U19 AG032438-0951, R01 AG052550, R01 AG068319, R01 AG053267). This work was supported by the Hope Center Alafi Neuroimaging Lab, a P30 Neuroscience Blueprint Interdisciplinary Center Core award (P30 NS057105), and a NIH Shared Instrumentation Grant to Washington University (S10 RR027552). This study was supported by the Dominantly Inherited Alzheimer Network (DIAN, NIH grants U19AG032438 and R01AG052550-01A1), the DIAN Trials Unit (DIAN-TU, NIH grants U01AG042791, U01AG042791-S1, R01AG046179, and R01AG53267-S1, as well as support from the Alzheimer's Association, GHR Foundation, an anonymous organization, the DIAN-TU Pharma Consortium, Eli Lilly and Company, Roche, Avid Radiopharmaceuticals, and CogState and Bracket), and the Neuroimaging Informatics and Analysis Center (P30NS098577).

Data availability Data access to the DIAN–TU trial data will follow the policies of the DIAN–TU data access policy [58], which complies with the guidelines established by the Collaboration for Alzheimer's

Prevention. Patient-related data not included in the paper were generated as part of a clinical trial and may be subject to patient confidentiality. Any data and materials that can be shared will be released via a data/material sharing agreement. Requests to access the DIAN–TU-001 trial data can be made at https://dian.wustl.edu/our-research/for-investigators/diantu-investigator-resources/. Data are available by request to the DIAN-Obs (https://dian.wustl.edu/our-research/observational-study/dian-observational-study-investigator-resources/data-request-terms-and-instructions/).

Code availability All code for data cleaning and analysis associated with the current submission is available upon request to the corresponding author and is provided as part of the replication package.

Declarations

Conflict of interest Washington University holds patents for one of the treatments (solanezumab), previously tested in the DIAN clinical trials. If solanezumab is approved as a treatment for Alzheimer's disease or Dominantly Inherited Alzheimer's Disease, Washington University will receive part of the net sales of solanezumab from Eli Lilly, which has licensed the patents related to solanezumab from Washington University. Johannes Levin reports speaker fees from Bayer Vital, Biogen, EISAI, TEVA, Zambon, Merck and Roche, consulting fees from Axon Neuroscience, EISAI and Biogen, author fees from Thieme medical publishers and W. Kohlhammer GmbH medical publishers and is inventor in a patent "Oral Phenylbutyrate for Treatment of Human 4-Repeat Tauopathies" (EP 23 156 122.6) filed by LMU Munich. In addition, he reports compensation for serving as chief medical officer for MODAG GmbH, is beneficiary of the phantom share program of MODAG GmbH and is inventor in a patent "Pharmaceutical Composition and Methods of Use" (EP 22 159 408.8) filed by MODAG GmbH, all activities outside the submitted work. Tammie Benzinger, MD, PhD, has received investigator initiated research funding from the NIH, the Alzheimer's Association, the Foundation at Barnes-Jewish Hospital, Siemens Healthineers and Avid Radiopharmaceuticals (a wholly-owned subsidiary of Eli Lilly and Company). She participates as a site investigator in clinical trials sponsored by Eli Lilly and Company, Biogen, Eisai, Jaansen, and Roche. She has served as a paid and unpaid consultant to Eisai, Siemens, Biogen, Janssen, and Bristol-Myers Squibb. John Morris consults for Barcelonaβeta Brain Research Foundation Scientific Advisory Board and Diverse VCID Observational Study Monitoring Board. He is on the advisory board for Cure Alzheimer's Fund Research Strategy Council and LEADS Advisory Board, University of Indiana. John Morris is funded by NIH grants # P30 AG066444; P01AG003991; P01AG026276. Neither John Morris nor his family owns stock or has equity interest (outside of mutual funds or other externally directed accounts) in any pharmaceutical or biotechnology company. Sandra Black reports grants or contracts from any entity (Contract Research: Genentech, Optina, Roche, Eli Lilly, Eisa/Biogen Idec, NovoNordisk, Lilly Avid, ICON; Peer Reviewed: Ontario Brain Institute, CIHR, Leducq Foundation, Heart and Stroke Foundation of Canada, NIH, Alzheimer's Drug Discovery Foundation, Brain Canada, Weston Brain Institute, Canadian Partnership for Stroke Recovery, Canadian Foundation for Innovation, Focused Ultrasound Foundation, Alzheimer's Association US, Department of National Defence, Montreal Medical International Kuwait, Queen's University, Compute Canada Resources for Research Groups, CANARIE, Networks of Centres of Excellence of Canada), consulting fees (Roche, Biogen, NovoNordisk, Eisai, Eli Lilly), payment or honoraria for lectures, presentations, speakers bureaus, manuscript writing or educational events (Biogen, Roche New England Journal Manuscript, Roche Models of Care Analysis in Canada in Submission, Eisai MRI Workshop), and participation on a Data Safety Monitoring Board or Advisory Board (Conference Board of Canada, World Dementia Council, University of Rochester Contribution to the Mission and Scientific Leadership of the Small Vessel VCID Biomarker Validation Consortium, National Institute of Neurological Disorders and Stroke). Lawrence Honig has received funding for consulting from Biogen, Eisai, Genentech/Roche, Medscape, and Prevail/Lilly, and has received institutional research funding from Abbvie, Acumen, Alector, AstraZeneca, Axovant, Avanir, Biogen, Bristol-Myer Squibb, Cognition, EIP, Eisai, Genentech/Roche, Janssen/Johnson & Johnson, Eli Lilly, Merck, Transposon, UCB, and Vaccinex. Richard Perrin's laboratory receives cost recovery funding from Biogen for tissue procurement and processing services related to ALS clinical trials.

Ethical approval The study was conducted in accordance with the Declaration of Helsinki (version 7) and the International Conference on Harmonization and Good Clinical Practice guidelines. Protocols for the study have received prior approval by the local Institutional Review Board (IRB) or Ethics Committee of each DIAN site and by the Washington University IRB for the Knight ADRC. The clinical trial registration number is NCT01760005.

Open Access This article is licensed under a Creative Commons Attribution-NonCommercial-NoDerivatives 4.0 International License, which permits any non-commercial use, sharing, distribution and reproduction in any medium or format, as long as you give appropriate credit to the original author(s) and the source, provide a link to the Creative Commons licence, and indicate if you modified the licensed material. You do not have permission under this licence to share adapted material derived from this article or parts of it. The images or other third party material in this article are included in the article's Creative Commons licence, unless indicated otherwise in a credit line to the material. If material is not included in the article's Creative Commons licence and your intended use is not permitted by statutory regulation or exceeds the permitted use, you will need to obtain permission directly from the copyright holder. To view a copy of this licence, visit http://creativecommons.org/licenses/by-nc-nd/4.0/.

References

1. Andersson E, Lindblom N, Janelidze S, Salvadó G, Gkanatsiou E, Söderberg L et al (2025) Soluble cerebral Aβ protofibrils link Aβ plaque pathology to changes in CSF Aβ42/Aβ40 ratios, neurofilament light and tau in Alzheimer's disease model mice. Nat Aging 5:366–375. https://doi.org/10.1038/s43587-025-00810-8
2. Bankhead P, Loughrey MB, Fernández JA, Dombrowski Y, McArt DG, Dunne PD et al (2017) QuPath: open source software for digital pathology image analysis. Sci Rep 7:16878. https://doi.org/10.1038/s41598-017-17204-5
3. Barthélemy NR, Toth B, Manser PT, Sanabria-Bohórquez S, Teng E, Keeley M et al (2022) Site-specific cerebrospinal fluid tau hyperphosphorylation in response to alzheimer's disease brain pathology: not all tau phospho-sites are hyperphosphorylated. J Alzheimer's Dis 85:415–429. https://doi.org/10.3233/JAD-210677
4. Bateman RJ, Xiong C, Benzinger TLS, Fagan AM, Goate A, Fox NC et al (2012) Clinical and biomarker changes in dominantly inherited Alzheimer's disease. N Engl J Med 367:795–804. https://doi.org/10.1056/NEJMoa1202753
5. Bateman RJ, Smith J, Donohue MC, Delmar P, Abbas R, Salloway S et al (2023) Two phase 3 trials of gantenerumab in early Alzheimer's disease. N Engl J Med 389:1862–1876. https://doi.org/10.1056/NEJMoa2304430
6. Bateman RJ, Li Y, McDade EM, Llibre-Guerra JJ, Clifford DB, Atri A et al (2025) Safety and efficacy of long-term gantenerumab

treatment in dominantly inherited Alzheimer's disease: an open-label extension of the phase 2/3 multicentre, randomised, double-blind, placebo-controlled platform DIAN-TU trial. Lancet Neurol 24:316–330. https://doi.org/10.1016/S1474-4422(25)00024-9
7. Benjamini Y, Hochberg Y (1995) Controlling the false discovery rate: a practical and powerful approach to multiple testing. J Roy Stat Soc: Ser B (Methodol) 57:289–300. https://doi.org/10.1111/j.2517-6161.1995.tb02031.x
8. Benzinger TLS, Blazey T, Jack CR, Koeppe RA, Su Y, Xiong C et al (2013) Regional variability of imaging biomarkers in autosomal dominant Alzheimer's disease. Proc Natl Acad Sci U S A 110:E4502-4509. https://doi.org/10.1073/pnas.1317918110
9. Beyreuther K, Masters CL (1991) Amyloid precursor protein (APP) and beta A4 amyloid in the etiology of Alzheimer's disease: precursor-product relationships in the derangement of neuronal function. Brain Pathol 1:241–251. https://doi.org/10.1111/j.1750-3639.1991.tb00667.x
10. Biel D, Brendel M, Rubinski A, Buerger K, Janowitz D, Dichgans M et al (2021) Tau-PET and in vivo Braak-staging as prognostic markers of future cognitive decline in cognitively normal to demented individuals. Alzheimers Res Ther 13:137. https://doi.org/10.1186/s13195-021-00880-x
11. Braak H, Braak E (1991) Neuropathological stageing of Alzheimer-related changes. Acta Neuropathol 82:239–259. https://doi.org/10.1007/BF00308809
12. Cairns NJ, Perrin RJ, Franklin EE, Carter D, Vincent B, Xie M et al (2015) Neuropathologic assessment of participants in two multi-center longitudinal observational studies: the Alzheimer disease neuroimaging initiative (ADNI) and the dominantly inherited Alzheimer network (DIAN). Neuropathology 35:390–400. https://doi.org/10.1111/neup.12205
13. Castellani RJ, Shanes ED, McCord M, Reish NJ, Flanagan ME, Mesulam M-M et al (2023) Neuropathology of anti-amyloid-β immunotherapy: a case report. J Alzheimer's Dis 93:803–813. https://doi.org/10.3233/JAD-221305
14. Chartier-Harlin MC, Crawford F, Houlden H, Warren A, Hughes D, Fidani L et al (1991) Early-onset Alzheimer's disease caused by mutations at codon 717 of the beta-amyloid precursor protein gene. Nature 353:844–846. https://doi.org/10.1038/353844a0
15. Chen CD, Holden TR, Gordon BA, Franklin EE, Li Y, Coble DW et al (2020) Ante- and postmortem tau in autosomal dominant and late-onset Alzheimer's disease. Ann Clin Transl Neurol 7:2475–2480. https://doi.org/10.1002/acn3.51237
16. Chen CD, Joseph-Mathurin N, Sinha N, Zhou A, Li Y, Friedrichsen K et al (2021) Comparing amyloid-β plaque burden with antemortem PiB PET in autosomal dominant and late-onset Alzheimer disease. Acta Neuropathol 142:689–706. https://doi.org/10.1007/s00401-021-02342-y
17. Chen CD, McCullough A, Gordon B, Joseph-Mathurin N, Flores S, McKay NS et al (2023) Longitudinal head-to-head comparison of 11C-PiB and 18F-florbetapir PET in a Phase 2/3 clinical trial of anti-amyloid-β monoclonal antibodies in dominantly inherited Alzheimer's disease. Eur J Nucl Med Mol Imaging. https://doi.org/10.1007/s00259-023-06209-0
18. Crehan H, Liu B, Kleinschmidt M, Rahfeld J-U, Le KX, Caldarone BJ et al (2020) Effector function of anti-pyroglutamate-3 Aβ antibodies affects cognitive benefit, glial activation and amyloid clearance in Alzheimer's-like mice. Alzheimer's Res Therapy 12:12. https://doi.org/10.1186/s13195-019-0579-8
19. Cummings J (2023) Anti-amyloid monoclonal antibodies are transformative treatments that redefine Alzheimer's disease therapeutics. Drugs 83:569–576. https://doi.org/10.1007/s40265-023-01858-9
20. van Dyck CH, Swanson CJ, Aisen P, Bateman RJ, Chen C, Gee M et al (2023) Lecanemab in early Alzheimer's disease. N Engl J Med 388:9–21. https://doi.org/10.1056/NEJMoa2212948
21. Fagan AM, Mintun MA, Mach RH, Lee S-Y, Dence CS, Shah AR et al (2006) Inverse relation between in vivo amyloid imaging load and cerebrospinal fluid Abeta42 in humans. Ann Neurol 59:512–519. https://doi.org/10.1002/ana.20730
22. Fischl B (2012) FreeSurfer. Neuroimage 62:774–781. https://doi.org/10.1016/j.neuroimage.2012.01.021
23. Glenner GG, Wong CW (1984) Alzheimer's disease: initial report of the purification and characterization of a novel cerebrovascular amyloid protein. Biochem Biophys Res Commun 120:885–890. https://doi.org/10.1016/S0006-291X(84)80190-4
24. Gordon BA, Blazey TM, Christensen J, Dincer A, Flores S, Keefe S et al (2019) Tau PET in autosomal dominant Alzheimer's disease: relationship with cognition, dementia and other biomarkers. Brain 142:1063–1076. https://doi.org/10.1093/brain/awz019
25. Hardy J, Allsop D (1991) Amyloid deposition as the central event in the aetiology of Alzheimer's disease. Trends Pharmacol Sci 12:383–388. https://doi.org/10.1016/0165-6147(91)90609-v
26. Hippius H, Neundörfer G (2003) The discovery of Alzheimer's disease. Dialogues Clin Neurosci 5:101–108
27. Honig LS, Vellas B, Woodward M, Boada M, Bullock R, Borrie M et al (2018) Trial of solanezumab for mild dementia due to Alzheimer's disease. N Engl J Med 378:321–330. https://doi.org/10.1056/NEJMoa1705971
28. Honig LS, Sun Y, Irizarry MC, Swanson CJ, Dhadda S, Charil A et al (2022) Neuropathological autopsy findings in an individual with Alzheimer's disease who received long-term treatment with lecanemab (BAN2401). Alzheimer's Dement 18:e069220. https://doi.org/10.1002/alz.069220
29. Hyman BT, Phelps CH, Beach TG, Bigio EH, Cairns NJ, Carrillo MC et al (2012) National institute on aging–Alzheimer's association guidelines for the neuropathologic assessment of Alzheimer's disease. Alzheimer's Dement 8:1–13. https://doi.org/10.1016/j.jalz.2011.10.007
30. Johnson ECB, Bian S, Haque RU, Carter EK, Watson CM, Gordon BA et al (2023) Cerebrospinal fluid proteomics define the natural history of autosomal dominant Alzheimer's disease. Nat Med 29:1979–1988. https://doi.org/10.1038/s41591-023-02476-4
31. Josephs KA, Murray ME, Whitwell JL, Tosakulwong N, Weigand SD, Petrucelli L et al (2016) Updated TDP-43 in Alzheimer's disease staging scheme. Acta Neuropathol 131:571–585. https://doi.org/10.1007/s00401-016-1537-1
32. Jucker M, Walker LC (2023) Alzheimer's disease: from immunotherapy to immunoprevention. Cell 186:4260–4270. https://doi.org/10.1016/j.cell.2023.08.021
33. Klein G, Delmar P, Voyle N, Rehal S, Hofmann C, Abi-Saab D et al (2019) Gantenerumab reduces amyloid-β plaques in patients with prodromal to moderate Alzheimer's disease: a PET substudy interim analysis. Alzheimers Res Ther 11:101. https://doi.org/10.1186/s13195-019-0559-z
34. Knopman DS, Hershey L (2023) Implications of the approval of lecanemab for Alzheimer disease patient care: incremental step or paradigm shift? Neurology 101:610–620. https://doi.org/10.1212/WNL.0000000000207438
35. Lopez OL, Hamilton R, Ikonomovic M, Mathis CA, Price JA, Becker JT et al (2009) IC-P-163: In vivo amyloid deposition and neuropathological findings after humanized amyloid β-specific monoclonal antibodies therapy in a patient with Alzheimer's disease. Alzheimer's Dement 5:P64–P65. https://doi.org/10.1016/j.jalz.2009.05.136
36. Mai JK, Majtanik M, Paxinos G (2015) Atlas of the human brain. Academic Press
37. Mintun MA, Lo AC, Duggan Evans C, Wessels AM, Ardayfio PA, Andersen SW et al (2021) Donanemab in early Alzheimer's disease. N Engl J Med 384:1691–1704. https://doi.org/10.1056/NEJMoa2100708

38. Morris JC, Aisen PS, Bateman RJ, Benzinger TLS, Cairns NJ, Fagan AM et al (2012) Developing an international network for Alzheimer research: the dominantly inherited Alzheimer network. Clin Investig (Lond) 2:975–984. https://doi.org/10.4155/cli.12.93
39. Nelson PT, Dickson DW, Trojanowski JQ, Jack CR, Boyle PA, Arfanakis K et al (2019) Limbic-predominant age-related TDP-43 encephalopathy (LATE): consensus working group report. Brain 142:1503–1527. https://doi.org/10.1093/brain/awz099
40. Nelson PT, Lee EB, Cykowski MD, Alafuzoff I, Arfanakis K, Attems J et al (2023) LATE-NC staging in routine neuropathologic diagnosis: an update. Acta Neuropathol 145:159–173. https://doi.org/10.1007/s00401-022-02524-2
41. Plowey ED, Bussiere T, Rajagovindan R, Sebalusky J, Hamann S, von Hehn C et al (2022) Alzheimer disease neuropathology in a patient previously treated with aducanumab. Acta Neuropathol 144:143–153. https://doi.org/10.1007/s00401-022-02433-4
42. Potter R, Patterson BW, Elbert DL, Ovod V, Kasten T, Sigurdson W et al (2013) Increased in vivo amyloid-β42 production, exchange, and loss in presenilin mutation carriers. Sci Transl Med 5:18ra977. https://doi.org/10.1126/scitranslmed.3005615
43. R Core Team (2021) R: a language and environment for statistical computing. R Foundation for Statistical Computing, Vienna, Austria
44. Robakis NK, Ramakrishna N, Wolfe G, Wisniewski HM (1987) Molecular cloning and characterization of a cDNA encoding the cerebrovascular and the neuritic plaque amyloid peptides. Proc Natl Acad Sci 84:4190–4194. https://doi.org/10.1073/pnas.84.12.4190
45. Ruifrok AC, Johnston DA (2001) Quantification of histochemical staining by color deconvolution. Anal Quant Cytol Histol 23:291–299
46. Salloway S, Farlow M, McDade E, Clifford DB, Wang G, Llibre-Guerra JJ et al (2021) A trial of gantenerumab or solanezumab in dominantly inherited Alzheimer's disease. Nat Med 27:1187–1196. https://doi.org/10.1038/s41591-021-01369-8
47. Scheltens P, Strooper BD, Kivipelto M, Holstege H, Chételat G, Teunissen CE et al (2021) Alzheimer's disease. Lancet 397:1577–1590. https://doi.org/10.1016/S0140-6736(20)32205-4
48. Schmidt U, Weigert M, Broaddus C, Myers G (2018) Cell Detection with Star-Convex Polygons. In: Frangi AF, Schnabel JA, Davatzikos C, Alberola-López C, Fichtinger G (eds) medical image computing and computer assisted intervention—MICCAI 2018. Springer International Publishing, Cham, pp 265–273
49. Schultz SA, Liu L, Schultz AP, Fitzpatrick CD, Levin R, Bellier J-P, Shirzadi Z, Joseph-Mathurin N, Chen CD, BenzingerTLS, Day GS, Farlow MR, Gordon BA, Hassenstab JJ, Jack CR, Jucker M, Karch CM, Lee J-H, Levin J, Perrin RJ, SchofieldPR, Xiong C, Johnson KA, McDade E, Bateman RJ, Sperling RA, Selkoe DJ, Chhatwal JP, Dominantly Inherited AlzheimerNetwork (2024) γ-Secretase activity, clinical features, and biomarkers of autosomal dominant Alzheimer's disease:cross-sectional and longitudinal analysis of the Dominantly Inherited Alzheimer Network observational study (DIANOBS).Lancet Neurol 23:913–924. https://doi.org/10.1016/S1474-4422(24)00236-9
50. Selkoe DJ (1991) The molecular pathology of Alzheimer's disease. Neuron 6:487–498. https://doi.org/10.1016/0896-6273(91)90052-2
51. Sevigny J, Chiao P, Bussière T, Weinreb PH, Williams L, Maier M et al (2016) The antibody aducanumab reduces Aβ plaques in Alzheimer's disease. Nature 537:50–56. https://doi.org/10.1038/nature19323
52. Sims JR, Zimmer JA, Evans CD, Lu M, Ardayfio P, Sparks J et al (2023) Donanemab in early symptomatic Alzheimer disease: the TRAILBLAZER-ALZ 2 randomized clinical trial. JAMA 330:512–527. https://doi.org/10.1001/jama.2023.13239
53. Solopova E, Romero-Fernandez W, Harmsen H, Ventura-Antunes L, Wang E, Shostak A et al (2023) Fatal iatrogenic cerebral β-amyloid-related arteritis in a woman treated with lecanemab for Alzheimer's disease. Nat Commun 14:8220. https://doi.org/10.1038/s41467-023-43933-5
54. Su Y, D'Angelo GM, Vlassenko AG, Zhou G, Snyder AZ, Marcus DS et al (2013) Quantitative analysis of PiB-PET with FreeSurfer ROIs. PLoS ONE 8:e73377. https://doi.org/10.1371/journal.pone.0073377
55. Swanson CJ, Zhang Y, Dhadda S, Wang J, Kaplow J, Lai RYK et al (2021) A randomized, double-blind, phase 2b proof-of-concept clinical trial in early Alzheimer's disease with lecanemab, an anti-Aβ protofibril antibody. Alzheimers Res Ther 13:80. https://doi.org/10.1186/s13195-021-00813-8
56. Tanzi RE, Gusella JF, Watkins PC, Bruns GAP, St George-Hyslop P, Van Keuren ML et al (1987) Amyloid β protein gene: cDNA, mRNA distribution, and genetic linkage near the alzheimer locus. Science 235:880–884. https://doi.org/10.1126/science.2949367
57. Wang G, Li Y, Xiong C, McDade E, Clifford DB, Mills SL et al (2022) Evaluation of dose-dependent treatment effects after mid-trial dose escalation in biomarker, clinical, and cognitive outcomes for gantenerumab or solanezumab in dominantly inherited Alzheimer's disease. Alzheimers Dement (Amst) 14:e12367. https://doi.org/10.1002/dad2.12367
58. Weninger S, Carrillo MC, Dunn B, Aisen PS, Bateman RJ, Kotz JD et al (2016) Collaboration for Alzheimer's prevention: principles to guide data and sample sharing in preclinical Alzheimer's disease trials. Alzheimers Dement 12:631–632. https://doi.org/10.1016/j.jalz.2016.04.001

Publisher's Note Springer Nature remains neutral with regard to jurisdictional claims in published maps and institutional affiliations.

Authors and Affiliations

Charles D. Chen[1] · Erin E. Franklin[1] · Yan Li[1] · Nelly Joseph-Mathurin[1] · Aime L. Burns[1] · Diana A. Hobbs[1] · Austin A. McCullough[1] · Stephanie A. Schultz[2] · Chengjie Xiong[1] · Guoqiao Wang[1] · Mario Masellis[3] · Ging-Yuek Robin Hsiung[4] · Serge Gauthier[5] · Sarah B. Berman[6] · Erik D. Roberson[7] · Lawrence S. Honig[8] · Roger Clarnette[9] · John M. Ringman[10] · James E. Galvin[11] · William Brooks[12,13] · Kazushi Suzuki[14] · Sandra Black[3,15,16,17,18] · Johannes Levin[19,20,21] · Neelum T. Aggarwal[22] · Mathias Jucker[23,24] · Matthew P. Frosch[2] · Julia K. Kofler[6] · Charles White III[25] · C. Dirk Keene[26] · Jie Chen[27] · Alisha Daniels[1] · Brian A. Gordon[1] · Laura Ibanez[1] · Celeste M. Karch[1] · Jorge Llibre-Guerra[1] · Eric McDade[1] · John C. Morris[1] · Charlene Supnet-Bell[1] ·

Ricardo F. Allegri[28] · Jae-Hong Lee[29] · Gregory S. Day[30] · Francisco Lopera[31] · Jee Hoon Roh[29] · Peter R. Schofield[32] · Susan Mills[1] · Tammie L. S. Benzinger[1] · Randall J. Bateman[1] · Richard J. Perrin[1] · For the DIAN-TU Study Team · For the DIAN-Obs Study Team

✉ Richard J. Perrin
rperrin@wustl.edu

[1] Washington University in St. Louis, St. Louis, MO, USA

[2] Massachusetts General Hospital, Boston, MA, USA

[3] Hurvitz Brain Sciences Research Program, Sunnybrook Research Institute, University of Toronto, Toronto, ON, Canada

[4] The University of British Columbia, Vancouver, BC, Canada

[5] McGill University, Montreal, QC, Canada

[6] University of Pittsburgh, Pittsburgh, PA, USA

[7] University of Alabama at Birmingham, Birmingham, AL, USA

[8] Taub Institute, Sergievsky Center, and Department of Neurology, Columbia University Irving Medical Center, New York, NY, USA

[9] University of Western Australia, Crawley, WA, Australia

[10] Keck School of Medicine of USC, Los Angeles, CA, USA

[11] University of Miami Miller School of Medicine, Atlantis, FL, USA

[12] Neuroscience Research Australia, Randwick, NSW, Australia

[13] University of New South Wales, Sydney, NSW, Australia

[14] National Defense Medical College, Saitama, Japan

[15] Division of Neurology, Department of Medicine, Sunnybrook Health Sciences Centre, Toronto, ON, Canada

[16] L.C. Campbell Cognitive Neurology Research Unit, Sunnybrook Health Sciences Centre, Toronto, ON, Canada

[17] Department of Neurology, University of Toronto, Toronto, ON, Canada

[18] Institute of Medical Science, University of Toronto, Toronto, ON, Canada

[19] Department of Neurology, LMU University Hospital, LMU Munich, Munich, Germany

[20] German Center for Neurodegenerative Diseases (DZNE), 81377, Munich, Germany

[21] Munich Cluster for Systems Neurology (SyNergy), Munich, Germany

[22] Rush University Medical Center, Chicago, IL, USA

[23] German Center for Neurodegenerative Diseases (DZNE), 72076 Tübingen, Germany

[24] Hertie Institute for Clinical Brain Research, University of Tübingen, Tübingen, Germany

[25] University of Texas Southwestern, Dallas, TX, USA

[26] University of Washington, Seattle, WA, USA

[27] University of Nebraska Medical Center, Omaha, NE, USA

[28] Instituto de Investigaciones Neurológicas Fleni, Buenos Aires, Argentina

[29] Korea University College of Medicine, Seoul, Korea

[30] Mayo Clinic, Jacksonville, FL, USA

[31] University of Antioquia, Medellin, Colombia

[32] Discipline of Psychiatry and Mental Health, University of New South Wales, Sydney, NSW, Australia